Lipid and Metabolite Deregulation in the Breast Tissue of Women Carrying *BRCA1* and *BRCA2* Genetic Mutations[1]

Saadallah Ramadan, PhD
Jameen Arm, BSc
Judith Silcock, RN
Gorane Santamaria, MD, PhD
Jessica Buck, BSc
Michele Roy, MD, FRCR
Kin Men Leong, MBBS, FRACR
Peter Lau, MBBS, FRACR
David Clark, MBBS, FRACS
Peter Malycha, MBBS, FRACS, FRCS
Carolyn Mountford, MSc, DPhil

Purpose: To use localized correlated spectroscopy (COSY) to assess for an altered biochemical state or states in breast tissue of women with *BRCA* gene mutations that potentially constitute preinvasive conditions.

Materials and Methods: Institutional review board approval was obtained. Participants provided written informed consent. In vivo localized COSY images were recorded at 3 T in the breast tissue of women carrying *BRCA1* ($n = 9$) or *BRCA2* ($n = 14$) gene mutations and were compared with images in healthy control subjects with no family history of breast cancer ($n = 10$). All participants underwent contrast material–enhanced MR imaging and ultrasonography (US). Statistical significance was calculated with the Mann-Whitney two-sided nonparametric test.

Results: No abnormality was recorded with MR imaging or US. Metabolite levels in the *BRCA1* cohort were reduced by 79% ($P = .014$) when compared with triglycerides level, and there was a 19% increase in lipid unsaturation and triglyceride levels ($P = .027$ and $P = .086$, respectively) when compared with cellular cholesterol level. Cholesterol level was reduced by 47% ($P = .027$) when compared with diallylic lipid level. Metabolite levels in the *BRCA2* cohort showed increased unsaturation of 21% ($P = .030$) relative to triglycerides level. Comparison of the *BRCA1* and *BRCA2* cohorts showed a 47% ($P = .002$) increase in cholesterol level in the *BRCA2* cohort when compared with diallylic lipid level and a 52% ($P = .003$) increase when compared with triglycerides level. Levels of diallylic lipid, unsaturated lipid, triglycerides, and terminal methyl on the acyl chain are reduced by 46% ($P = .002$), 57% ($P = .003$), 66% ($P = .003$), and 29% ($P = .010$), respectively, when compared with cholesterol level.

Conclusion: Localized COSY recorded significant changes in women with *BRCA1* and *BRCA2* gene mutations when compared with control subjects. If these changes are ultimately proven to be a premalignant stage, this method may prove useful in screening.

© RSNA, 2015

BRCA1 and BRCA2 genes belong to the tumor suppressor family, and mutations cause an increased risk for breast cancer (1). A woman carrying the BRCA1 or BRCA2 mutation has approximately a 3% risk of developing breast cancer before the age of 30 years. This risk increases to almost 50% at 50 years of age, and increases again to 50%–80% at 70 years of age (2). Women carrying BRCA gene mutations can develop cancer within months of negative findings at mammography, magnetic resonance (MR) imaging, or ultrasonography (US) screening, leading to the hypothesis that a preinvasive state or states may exist that cannot be identified with the current diagnostic modalities.

The foundation used to identify chemical changes associated with tumor development and progression was derived by using MR spectroscopy to study cell models and biopsies (3,4). The MR spectroscopy method allows one to record those molecules that are mobile on the MR time scale (5) and thus in active pools often associated with disease. Cell models of tumor development and progression were important in correlating MR spectral changes with specific biologic and genetic characteristics (6–8). The earliest biomarkers of the premalignant state or states were MR-detectable lipids and cholesterol, where the chemical properties remain constant whether in a lipoprotein, cell, or organ. In parallel, the causes of the aberrant choline phospholipid metabolism in patients with breast cancer were documented (9).

In a one-dimensional MR spectrum, the resonances overlap, often providing ambiguous assignments. Two-dimensional (2D) correlated spectroscopy (COSY), which is used to measure covalent linkages between protons in a molecule, separates the composite resonances in a second frequency, allowing assignment and identification of the chemical change. To better understand the process of tumor development and how lipids and metabolite profiles changed, 2D COSY was compared with the chemical analyses of whole cells and purified membranes of models with established genetic and cell biologic characteristics (7). Lipid and cholesterol levels were shown to be the first markers of cellular instability and were considered the earliest of the premalignant changes.

With improvements in MR magnet and coil technology, it became possible to record some of this information in vivo with a clinical imager. Thomas and colleagues used 2D localized COSY to support the concept that the lipid level was a diagnostic marker of malignancy (10). The 2D localized COSY has since enabled noninvasive diagnosis and chemical assessment of glioma (11), where the results were comparable with the information from cell models.

We hypothesized that women with BRCA gene mutations have altered chemistry reflective of a preinvasive state or states, and in vivo 2D localized COSY could offer a means to screen these women. The purpose of this study was to assess for an altered biochemical state or states in the breast tissue of women with BRCA gene mutations that potentially constitute preinvasive conditions.

Materials and Methods

Patients and Healthy Control Subjects

The study was approved by the Hunter New England Area Health Ethics Committee, and all patients and control subjects provided written informed consent.

The recruitment of the BRCA cohorts was through The Breast and Endocrine Centre in Gateshead, New South Wales, Australia, where genetic testing was performed as part of the routine clinical management. Nine women with a genetically confirmed BRCA1 mutation (age range, 41–62 years; median age, 54 years) and 14 women with a genetically confirmed BRCA2 mutation (age range, 25–70 years; median age, 52.5 years) were recruited. Nine women (five with BRCA1 mutations, four with BRCA2 mutations) were found to have had cysts or lesions. In these women, we examined the apparently healthy and unaffected

---

Advances in Knowledge

- Women carrying BRCA gene mutations have metabolic deregulations in their breast tissue that may be precursors to malignant transformation.

- Women carrying BRCA1 gene mutations exhibited a reduction of 79% in metabolite level, while both lipid unsaturation and triglyceride levels increased by 19%.

- Women carrying BRCA2 gene mutations showed an increased lipid unsaturation of 21%.

- The metabolic changes in women carrying BRCA1 gene mutations are different from those in women carrying BRCA2 gene mutations, with a 47% increase in cholesterol level recorded in those with BRCA2 gene mutations.

Implication for Patient Care

- If confirmed in larger populations, it is possible that the information provided by localized correlated spectroscopy will allow women carrying BRCA gene mutations an objective means with which to monitor the extent of biochemical changes taking place in their breast tissue.

breast. All women were examined by a breast surgeon (D.C.) prior to MR imaging. A healthy control cohort was recruited from the wider community in the Hunter region, New South Wales, Australia. The control subjects had no family history of breast cancer ($n = 10$; age range, 34–68 years; median age, 47.5 years).

MR Imaging and Spectroscopy

The study was performed with either a 3-T Skyra MR imager (Siemens, Erlangen, Germany) and use of a 70-cm-diameter body coil for signal excitation or a 3-T Prisma MR imager (Siemens) and use of a 60-cm-diameter body coil for excitation. A two-cavity 16-channel breast coil was used for signal reception (RAPID Biomedical, Rimpar Germany).

Breast MR Imaging

Routine breast T2- and T1-weighted MR imaging was performed. This consisted of a localizer sequence (repetition time msec/echo time msec, 6/2.61; section thickness, 7 mm; field of view, 400 mm), an axial T1-weighted three-dimensional fast low-angle shot non–fat-saturated radial sequence (5.43/2.46; flip angle, 20°; section thickness, 2 mm; field of view, 300 mm; matrix, 448 × 448 mm), an axial T2-weighted turbo spin-echo sequence (4970/95; section thickness, 2 mm; field of view, 300 mm; matrix, 448 × 448 mm), and an axial T1-weighted three-dimensional fast low-angle shot dynamic series (4.54/1.73; flip angle, 10°; section thickness, 1.2 mm; field of view, 300 mm; matrix, 448 × 448 mm) with one pre- and five postcontrast (Omniscan; GE Healthcare, Oslo, Norway) time points. Injection of this neutral chelate was performed in all patients but was not performed in the healthy control subjects. Four patients in the *BRCA1* cohort had undergone 2D COSY prior to and after contrast agent administration to ascertain if the contrast agent affected the spectral results. The MR images were examined independently by radiologists in three different practices with 10, 15, and 30 years of experience in breast imaging (K.S.Y., G.S., and P.L., respectively).

Figure 1
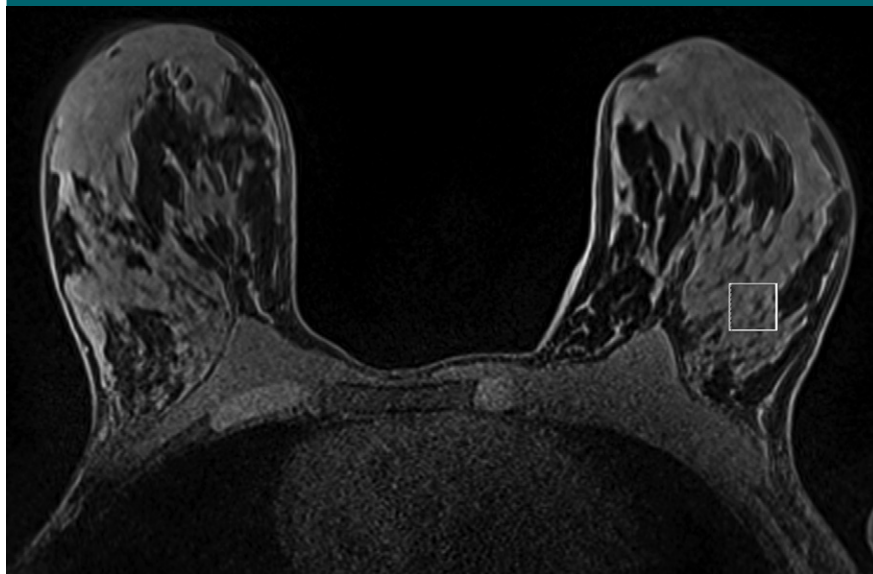
Figure 1: Unenhanced image shows region of interest placement in a 30-year-old control subject. This is the spectroscopic voxel location from which 2D localized COSY data were collected. The experimental conditions were as described previously.

Localized COSY 2D MR Spectroscopy

Anatomic MR imaging was used to position the 15 × 15 × 15 mm voxel in the lower left outer quadrant midway between fibroglandular and fat tissues. If the woman had undergone previous surgery in the left breast, the voxel was placed in the right breast in the outer quadrant (Fig 1). Voxel placement was the same for all participants, and voxels were placed by one of the radiologists. Localized shimming was performed with automatic adjustment of zero- and first-order shim gradients by using the automatic B_0-field mapping technique automatic shimming algorithm (Siemens) (12), followed by manual adjustment of zero-order shim gradients to achieve width of water at half maximum of 40 Hz or more.

The localized COSY sequence was applied with an initial echo time of 30 msec, repetition time of 1.5 seconds, eight signal averages per increment, a bandwidth of 2000 Hz, a T1 increment of 0.8 msec, and a vector size of 1024 points; the radiofrequency offset frequency was set on 3.2 ppm, and increments were 64. The water suppression enhanced through T1

effects (or WET) technique (13) was applied. Processing was undertaken, as previously reported (11). The assignment of protons to the triglyceride molecule is shown in Figure 2, and the assignment of protons to the cholesterol molecule is shown in Figure 3. Cross and diagonal peak volumes were measured with Felix software (San Diego, Calif) (14), with the $(CH_2)_n$ diagonal peak at 1.30 ppm as the internal chemical shift reference. The measurement of peak volumes was undertaken by prescribing a box on top of the area of interest, and the aforementioned software enabled us to measure the volume of signal under this box. The same box sizes were applied to all spectra to reduce operator variability. Because of the absence of a reliable internal concentration standard, the ratios were calculated for all localized COSY spectra with respect to the following peaks: (5.30, 5.30) ppm, (2.75, 2.75) ppm, (1.30, 1.30) ppm, and (4.25, 4.25) ppm. The unsaturation index was also measured and calculated by using cross peaks at (5.30, 2.75) ppm and (5.30, 2.05) ppm, as reported by Velan et al (15). Five authors are listed on a

Radiology
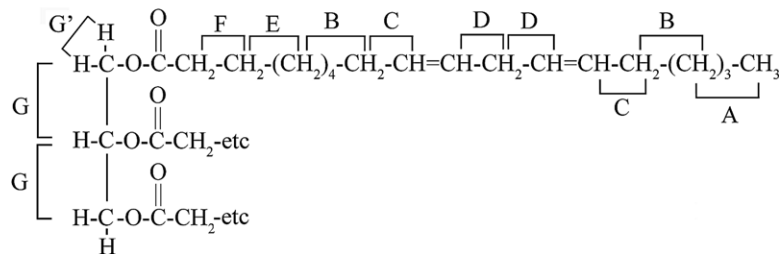
Figure 2

Figure 2: Diagram of a fatty acyl chain, with the associated spectroscopic cross peaks *(A–G')* labeled.

Figure 3
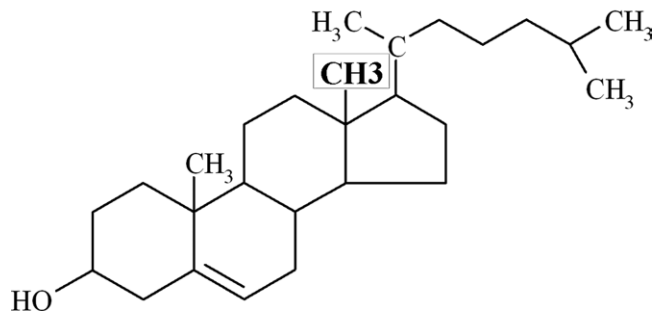
Figure 3: Diagram of the structure of a cholesterol molecule, with the methyl group used for spectroscopic detection in bold.

pending patent regarding this technique (S.R., G.S., D.C., P.M., C.M.).

Statistical Analysis

Evaluation of statistical significance was undertaken by using Excel 2010 (Microsoft, Redmond, Wash) and the Real Statistics Resource Pack (16). Statistical significance was calculated for all assigned cross and diagonal peaks with a two-tailed nonparametric Mann-Whitney test since data did not pass a normal distribution test. Biomarker resonance ratios with $P \leq .05$ were identified and listed. The statistical findings were not corrected for multiple comparisons since this was a small exploratory study.

Results

Clinical Assessment

None of the breast tissue examined with the 2D localized COSY method exhibited any indication of abnormality at MR imaging or US. All breast images were rated as Breast Imaging Reporting and Data System category 1 or 2.

Effect of Contrast Agent Administration on 2D COSY

Four women with *BRCA1* gene mutations were examined before and after contrast agent administration by using 2D localized COSY, and no variation in cross peak volume greater than 8% was recorded for any of the data sets. This is considerably smaller than the changes recorded between cohorts.

2D Localized COSY Assessment

The COSY spectra, recorded in women with either a *BRCA1* gene mutation or a *BRCA2* gene mutation, are compared with a spectrum from a healthy breast in Figure 4. The cross peaks are assigned, as per Figures 2 and 3.

When we compared women with *BRCA1* gene mutations with control subjects for peak volumes versus triglycerides level (4.25, 4.25 ppm), no changes were recorded in the level of lipid unsaturation; however, the level of the composite resonance containing the metabolites choline, glycine, and myo-inositol decreased by 79% ($P = .014$). When compared with the cholesterol level, women with *BRCA1* gene mutations showed an increase in lipid unsaturation and triglyceride levels of 19%, with P values of .027 and .086, respectively. When compared with the diallylic lipid level, the substrate metabolite resonance (choline, glycine, and myo-inositol) level was reduced by 98% ($P = .018$); the glycerol, glutamine or glutamate, and glucose composite was reduced by 70% ($P = .072$); and the cholesterol level was reduced by 47% ($P = .027$) (Table).

When we compared the *BRCA2* cohort with control subjects relative to triglyceride levels (4.25, 4.25 ppm), there were significant increases in the level of unsaturation of 21% and 21%, with P values of .030 and .040, respectively. When we compared cholesterol levels in the *BRCA2* cohort with the triglycerides level and the terminal methyl level of the lipid acyl chains in control subjects, decreases of 55% ($P = .069$) and 50% ($P = .053$), respectively, were recorded.

Comparison of the *BRCA1* and *BRCA2* cohorts showed a 47% ($P = .002$) increase in cholesterol level in the *BRCA2* cohort when compared with the diallylic lipid level and a 52% ($P = .003$) increase when compared with the triglycerides level. When compared with the cholesterol level, the diallylic lipid, cross peak D, triglyceride, and cross peak A levels are reduced by 46% ($P = .002$), 57% ($P = .003$), 66% ($P = .003$), and 29% ($P = .010$), respectively, showing that the unsaturated triglyceride level is reduced in relation to cholesterol level in the *BRCA2* cohort.

Discussion

Results from this study show biochemical changes that may indicate a

Figure 4

a.

b.
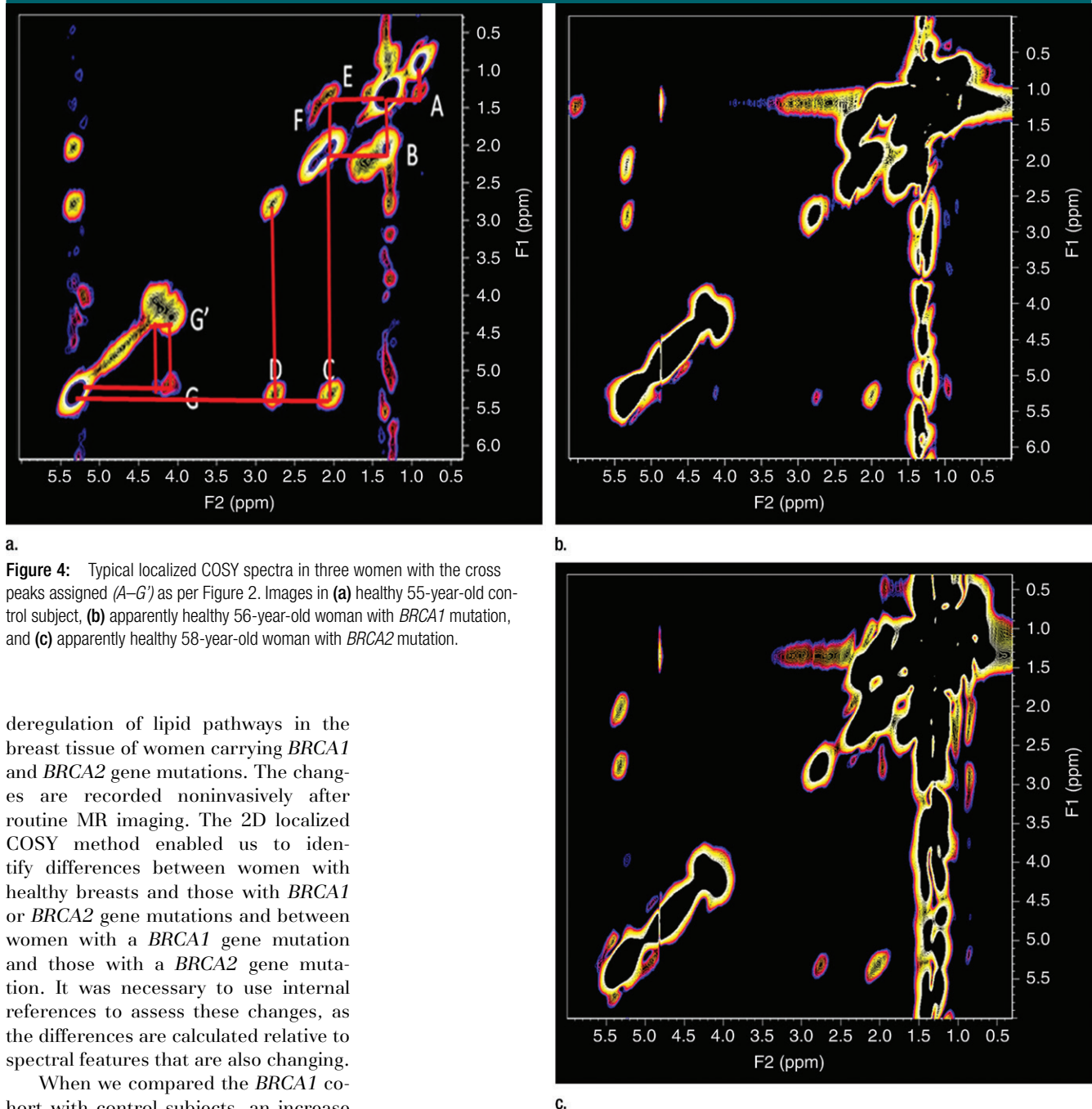
Figure 4: Typical localized COSY spectra in three women with the cross peaks assigned *(A–G')* as per Figure 2. Images in **(a)** healthy 55-year-old control subject, **(b)** apparently healthy 56-year-old woman with *BRCA1* mutation, and **(c)** apparently healthy 58-year-old woman with *BRCA2* mutation.

c.

deregulation of lipid pathways in the breast tissue of women carrying *BRCA1* and *BRCA2* gene mutations. The changes are recorded noninvasively after routine MR imaging. The 2D localized COSY method enabled us to identify differences between women with healthy breasts and those with *BRCA1* or *BRCA2* gene mutations and between women with a *BRCA1* gene mutation and those with a *BRCA2* gene mutation. It was necessary to use internal references to assess these changes, as the differences are calculated relative to spectral features that are also changing.

When we compared the *BRCA1* cohort with control subjects, an increase in the glycerol backbone of triglycerides was accompanied by an increase in unsaturation of the fatty acyl chains. The concentration of composite metabolite resonances was also reduced. For the *BRCA2* cohort, changes were consistent with an increase in the unsaturation of the fatty acyl chains relative

to triglycerides, but the composite metabolite resonances did not appear to have been affected. This suggests that there are multiple populations of lipids altering relative to one another both in women with *BRCA1* mutations and in women with *BRCA2* mutations.

The increase in cholesterol level in the *BRCA2* cohort indicates lipid pathways are affected differently in the two different gene mutations. In our earlier studies of the chemical analysis of purified plasma membranes of tumor cell models, the unsaturation was totally

Summary of Differences between the *BRCA1*, *BRCA2*, and Healthy Control Cohorts

F2, F1 ppm	Chemical Species/Fragment	Peak Volume Ratio to Chemical Species						P Value		
		Healthy Cohort		BRCA1 Cohort		BRCA2 Cohort		Healthy Cohort vs BRCA1 Cohort	Healthy Cohort vs BRCA2 Cohort	BRCA1 Cohort vs BRCA2 Cohort
		Median	Interquartile Range	Median	Interquartile Range	Median	Interquartile Range			
		Triglyceride Backbone (4.25, 4.25) ppm								
2.75, 2.75	Lipid=CH-CH2-CH =	0.359	0.00878	0.376	0.0905	0.461	0.122	.624 (12.0)	.030 (21.1)	.166 (10.4)
2.02, 2.02	Lipid=CH-CH2-CH2	1.476	0.423	1.451	0.219	1.801	0.430	>.99 (−1.5)	.061 (16.3)	.020 (17.5)
2.02, 1.30	LipidCross peak E	1.178	0.317	1.155	0.112	1.385	0.345	.935 (1.7)	.040 (20.6)	.032 (19.1)
3.50, 3.50	Choline, glycine, myo-inositol	0.00307	0.00480	0.00321	0.00225	0.00669	0.00720	.014 (−78.9)	.725 (19.2)	.051 (54.8)
0.70, 0.70	Cholesterol methyl group	0.108	0.0642	0.0751	0.0249	0.119	0.0725	.327 (−30.9)	.069 (37.2)	.003 (52.0)
		=CH-CH2-CH =(diallylic lipid) (2.75, 2.75) ppm								
4.25, 4.25	Lipid–CH2-*O*-CO (triglyceride backbone)	2.822	0.936	2.656	0.641	2.170	0.648	.624 (−14.4)	.030 (−29.9)	.166 (−13.6)
3.50, 3.50	Choline, glycine, myo-Inositol	0.0134	0.0162	0.00969	0.00586	0.0170	0.0206	.018 (−97.6)	.770 (−4.0)	.115 (47.3)
3.70, 3.70	Glycerol, glutamine, glucose	0.00807	0.00961	0.00666	0.00252	0.0119	0.0118	.072 (−70.3)	.520 (−10.7)	.571 (41.6)
0.90, 1.30	LipidCross peak A	3.720	1.636	3.245	1.101	2.970	0.728	.253 (−20.1)	.026 (−27.2)	.488 (−6.0)
0.70, 0.70	Cholesterol methyl group	0.345	0.138	0.214	0.0438	0.336	0.162	.027 (−47.1)	.412 (22.3)	.002 (47.2)
		Cholesterol Methyl Group (0.70, 0.70) ppm								
2.75, 2.75	Lipid=CH-CH2-CH =	3.238	1.329	4.665	0.941	2.987	1.314	.027 (18.9)	.412 (−18.1)	.002 (−45.6)
5.30, 2.75	LipidCross peak D	0.942	0.846	1.765	0.428	0.940	0.498	.060 (14.4)	.598 (−34.4)	.003 (−57.0)
4.25, 4.25	Lipid–CH2-*O*-CO (triglyceride backbone)	9.220	7.741	13.310	4.263	6.453	3.030	.327 (6.2)	.069 (−55.4)	.003 (−65.8)
0.90, 1.30	LipidCross peak A	13.365	9.689	17.805	7.962	8.174	4.444	.513 (1.1)	.053 (−50.5)	.010 (−28.8)
4.25, 5.30	LipidCross peak G	0.821	0.586	1.241	1.013	0.516	0.286	.086 (19.3)	.160 (−31.0)	.004 (−62.3)

Note.—Data in parentheses are the percentage difference.

within the triglyceride population (8). The *BRCA1* group showed an apparent increase in triglyceride and unsaturation levels.

Changes to fatty acyl chain unsaturation were consistent with those in the literature (17,18), where an increase in the expression of fatty-acid synthase is seen in cancer pathogenesis (19). The first step of fatty acid biosynthesis requires activation of acetyl-CoA to malonyl-CoA catalyzed by acetyl-CoA carboxylase. The acetyl and malonyl groups are then coupled to the acyl carrier protein domain of the fatty acid synthase. Unsaturation is catalyzed by fatty acyl-CoA desaturases to produce monounsaturated fatty acids. Fatty acyl-CoA desaturases catalyze the synthesis of highly unsaturated fatty acids from essential polyunsaturated fatty acids. Several studies have shown that tumor cells reactivate de novo lipid synthesis (19).

An important observation was the alteration of cholesterol levels in the *BRCA2* cohort. This suggests that these women have cholesterol deregulation occurring in addition to fatty acyl chain unsaturation and increased triglyceride levels. When compared with cell model studies, each may constitute yet another part of the premalignant process.

The appearance of cholesterol in breast tissue in the in vivo study is directly comparable with a colorectal cell model where two adenoma cell lines were compared with four malignant cell lines (7). The nontumorigenic PC/AA adenoma cell line had a normal karyotype at low passage number, and *K-ras* mutations had been detected both in early and later passages (20). The 2D COSY of this cell line showed the unsaturated triglyceride but no cholesterol. The next cell line in the model PC/AACl had marker chromosome 1 and other abnormalities, including loss of one chromosome 18. This is of interest, since loss or mutation of the tumor suppressor *DCC* gene, located on chromosome 18q, has been implicated in tumorigenesis (21). Also PC/AACl was nontumorigenic in nude mice. The 2D COSY of PC/AACl showed both unsaturated triglyceride and cholesterol.

Thus, by analogy, those women without cholesterol compare directly with PC/AA and those with cholesterol present in their spectrum fit the PC/AA1 profile (7). This suggests that tumors in women with the PC/AA1 profile may be one step closer to malignancy.

The mevalonate pathway facilitates synthesis of cholesterol (22). The first steps of cholesterol biosynthesis involve condensation of acetyl-CoA with acetoacetyl-CoA to form 3-hydroxy-3-methylglutaryl-CoA. The reduction of 3-hydroxy-3-methylglutaryl-CoA to mevalonate represents the rate-limiting reaction of the cholesterol synthesis pathway and is highly regulated. Interestingly, this reductase is the target for a class of cholesterol-lowering drugs, the statins, which show antiproliferative activity in several cancer cell lines, including breast cancer cells (23).

These results suggest that MR-observable cholesterol in the breast tissue of patients with a *BRCA* mutation is a biomarker that potentially indicates a higher probability of developing a lesion that progresses to malignancy. The detection of cholesterol with 2D localized COSY used to analyze the breast parenchyma of patients with *BRCA* mutations might enable identification of a group at higher risk. This requires a larger patient cohort to confirm these findings and the opportunity to monitor women who proceed through this adenoma to carcinoma sequence.

The reduction in the levels of the metabolites (glycerol, glycine, and/or inositol) in the breast tissue of women with a *BRCA1* mutation is intriguing and requires further experimentation to determine which molecule or molecules are altered. It does, however, suggest metabolic activity is abnormal and that some of these molecules have been used up as a substrate. For example, glycine is known to fuel cancer cells (24), while inositol hexaphosphate blocks proliferation of human breast cancer (25).

Importantly, these results indicate that *BRCA1* and *BRCA2* gene mutations differ in the order in which lipid deregulation and substrate usage occur.

It has been documented elsewhere that women with a *BRCA2* mutation survive longer than women with a *BRCA1* mutation. These results suggest that there are biochemical differences that may explain this difference.

A larger study is now underway in two states in Australia to reach the required cohort size to verify the smallest change recorded (ie, the decrease in the substrates in the *BRCA2* category). In addition, those women who have agreed to participate in this study are offered an MR examination with the 2D localized COSY protocol every 6 months. The return rate is high, and we expect to be in a position to monitor the adenocarcinoma sequence in some of these participants.

A limitation to this study was the small number of women in each category and the fact that we did not correct for multiple comparisons given the exploratory nature of the study. The analysis would also benefit from an informatics approach (26–28), since the current calculations are based on resonance ratios of lipids, which are altering. Another limitation was the small number of patients studied before and after contrast material administration. Serum lipid levels were not measured. Some patients were on lipid-lowering drugs; thus, the effect on the spectra needs to be examined in the ongoing study. Future studies will include the measurement of serum lipoprotein and cholesterol levels. The metabolic alterations that we describes are associated with cancer metabolism but were not proved in this study to indicate presence of active disease.

In summary, despite no evidence of any changes to breast tissue from current imaging modalities, in vivo 2D localized COSY MR spectroscopy enables identification of biochemical abnormalities that may represent pre-invasive changes in the breast tissue of women carrying the *BRCA1* or *BRCA2* gene mutation. These differences are supported by results from a cell model of tumorigenesis. The changes include alterations to the amount and saturation of triglycerides, cholesterol, and

Radiology

metabolic substrates that precede the activation of choline metabolism through the choline kinase and phospholipase C over expression. Importantly, *BRCA1* differs from *BRCA2*.

References

1. Health Quality Ontario. Cancer screening with digital mammography for women at average risk for breast cancer, magnetic resonance imaging (MRI) for women at high risk: an evidence-based analysis. Ont Health Technol Assess Ser 2010;10(3):1–55.

2. Veltman J, Mann R, Kok T, et al. Breast tumor characteristics of BRCA1 and BRCA2 gene mutation carriers on MRI. Eur Radiol 2008;18(5):931–938.

3. Mountford CE, Doran S, Lean CL, Russell P. Proton MRS can determine the pathology of human cancers with a high level of accuracy. Chem Rev 2004;104(8):3677–3704.

4. Mountford C, Lean C, Malycha P, Russell P. Proton spectroscopy provides accurate pathology on biopsy and in vivo. J Magn Reson Imaging 2006;24(3):459–477.

5. Thomas MA, Yue K, Binesh N, et al. Localized two-dimensional shift correlated MR spectroscopy of human brain. Magn Reson Med 2001;46(1):58–67.

6. Mackinnon WB, Dyne M, Hancock R, Grant AJ, Russell P, Mountford CE. Malignancy-related characteristics of wild type and drug-resistant Chinese hamster ovary cells. Pathology 1993;25(3):268–276.

7. Mackinnon WB, Huschtscha L, Dent K, Hancock R, Paraskeva C, Mountford CE. Correlation of cellular differentiation in human colorectal carcinoma and adenoma cell lines with metabolite profiles determined by 1H magnetic resonance spectroscopy. Int J Cancer 1994;59(2):248–261.

8. Mackinnon WB, May GL, Mountford CE. Esterified cholesterol and triglyceride are present in plasma membranes of Chinese hamster ovary cells. Eur J Biochem 1992;205(2):827–839.

9. Glunde K, Bhujwalla ZM, Ronen SM. Choline metabolism in malignant transformation. Nat Rev Cancer 2011;11(12):835–848.

10. Thomas MA, Lipnick S, Velan SS, et al. Investigation of breast cancer using two-dimensional MRS. NMR Biomed 2009;22(1):77–91.

11. Ramadan S, Andronesi OC, Stanwell P, Lin AP, Sorensen AG, Mountford CE. Use of in vivo two-dimensional MR spectroscopy to compare the biochemistry of the human brain to that of glioblastoma. Radiology 2011;259(2):540–549.

12. Mountford CE, Schuster C, Baltzer PA, Malycha P, Kaiser WA. MR spectroscopy in the breast clinic is improving. Eur J Radiol 2012;81(1 Suppl 1):S104–S106.

13. Ogg RJ, Kingsley PB, Taylor JS. WET, a T1- and B1-insensitive water-suppression method for in vivo localized 1H NMR spectroscopy. J Magn Reson B 1994;104(1):1–10.

14. Accelrys. Felix NMR 2007 Version. http://www.felixnmr.com/products.htm. Published 2007. Accessed July 2012.

15. Velan SS, Durst C, Lemieux SK, et al. Investigation of muscle lipid metabolism by localized one- and two-dimensional MRS techniques using a clinical 3T MRI/MRS scanner. J Magn Reson Imaging 2007;25(1):192–199.

16. Zaiontz C. Real Statistics Resource Pack Version 2.10.1. Real Statistics. http://www.real-statistics.com/free-download/real-statistics-resource-pack/real-statistics-resource-pack-macintosh/. Published 2014. Accessed August 2014.

17. Li JN, Mahmoud MA, Han WF, Ripple M, Pizer ES. Sterol regulatory element-binding protein-1 participates in the regulation of fatty acid synthase expression in colorectal neoplasia. Exp Cell Res 2000;261(1):159–165.

18. Yoon S, Lee MY, Park SW, et al. Up-regulation of acetyl-CoA carboxylase alpha and fatty acid synthase by human epidermal growth factor receptor 2 at the translational level in breast cancer cells. J Biol Chem 2007;282(36):26122–26131.

19. Menendez JA, Lupu R. Fatty acid synthase and the lipogenic phenotype in cancer pathogenesis. Nat Rev Cancer 2007;7(10):763–777.

20. Farr CJJ, Marshall CJ, Easty DJ, Wright NA, Powell SC, Paraskeva C. A study of ras gene mutations in colonic adenomas from familial polyposis coli patients. Oncogene 1988;3(6):673–678.

21. Fearon ER, Vogelstein B. A genetic model for colorectal tumorigenesis. Cell 1990;61(5):759–767.

22. Chang TY, Chang CC, Ohgami N, Yamauchi Y. Cholesterol sensing, trafficking, and esterification. Annu Rev Cell Dev Biol 2006;22:129–157.

23. Rao S, Lowe M, Herliczek TW, Keyomarsi K. Lovastatin mediated G1 arrest in normal and tumor breast cells is through inhibition of CDK2 activity and redistribution of p21 and p27, independent of p53. Oncogene 1998;17(18):2393–2402.

24. Chenette EJ. Glycine fuels cancer cells. Nat Cell Biol 2012;14(7):658.

25. Vucenik I, Ramakrishna G, Tantivejkul K, Anderson LM, Ramljak D. Inositol hexaphosphate (IP6) blocks proliferation of human breast cancer cells through a PKCdelta-dependent increase in p27Kip1 and decrease in retinoblastoma protein (pRb) phosphorylation. Breast Cancer Res Treat 2005;91(1):35–45.

26. Somorjai RL. Creating robust, reliable, clinically relevant classifiers from spectroscopic data. Biophys Rev 2009;1(4):201–211.

27. Cocuzzo D, Lin A, Ramadan S, Mountford C, Keshava N. Algorithms for characterizing brain metabolites in two-dimensional in vivo MR correlation spectroscopy. Conf Proc IEEE Eng Med Biol Soc 2011;2011:4929–4934.

28. Cocuzzo D, Lin A, Stanwell P, Mountford C, Keshava N. In vivo brain magnetic resonance spectroscopy: a measurement of biomarker sensitivity to post-processing algorithms. IEEE J Transl Eng Health Med 2014;2(1):1–17.